

Stable particle acceleration in co-axial plasma channels

Alexander Pukhov and John P. Farmer

Institut für Theoretische Physik I, Universität Düsseldorf, 40225 Germany

Plasma wakefields [1] offer a potential basis for novel high-energy particle accelerators [2] due to the high field gradients plasma can support. In this work, we investigate the use of a pre-formed plasma channel for the controlled monoenergetic acceleration of a witness [3]. Typically acceleration in such hollow plasma channels, as well as in dielectric waveguides [4], is limited by the beam breakup (BBU) instability [5–7]. Using three-dimensional particle-in-cell simulations, we show for the first time that BBU can be avoided by using a co-axial plasma filament in the hollow channel. The high-current electron driver scatters electrons from the on-axis filament, leaving an ion column which focuses both the driver and the trailing electron witness bunch. The slow pinching of the ion column leads to a strong dynamic chirp of the effective betatron frequency along the beam length, preventing growth of the BBU instability. We show that this stable configuration allows transformer ratios as high as 10 to be achieved with an energy efficiency of 40%. The co-axial channel is also suitable for high-gradient acceleration of donut-shaped positron bunches.

Plasma-based accelerators consist of a driver which excites a plasma wake, which is in turn used to accelerate a trailing witness bunch. The driver can be either an intense laser pulse [8] or a charged particle bunch [9]. In this work, we focus on the latter. One can use short - shorter than the plasma period - drive bunches in quasi-linear [10] or blow-out [11, 12] regimes. Alternatively, one may harness the self-modulation of longer bunches in plasma [13, 14]. For the accelerating medium, one may choose either uniform plasma [9], or a pre-formed plasma channel [15]. Each of these regimes has its own particular advantages and drawbacks.

Perhaps the most promising accelerating scheme is that of the hollow plasma channel [3]. A radially symmetric drive bunch in a cylindrical channel does not generate any focusing or defocusing fields, which would guarantee the conservation of the transverse emittance of the witness [16]. Further, the accelerating field is uniform across the hollow channel, allowing monoenergetic acceleration. A high quality witness bunch is vital for a number of applications, such as future high-energy colliders [17] or XFEL machines [18]. Thus, hollow-plasma-channel acceleration appears the perfect candidate for next-generation particle accelerators.

Unfortunately, hollow plasma channels suffer from a severe drawback - the beam breakup (BBU) instability [5, 6]. As a charged bunch propagates in a hollow channel, plasma

electrons in the channel wall respond. The resulting space-charge results in an attractive force between the bunch and the wall. The plasma response increases as the bunch moves towards the wall, increasing the attractive force. This instability manifests as a hosing of the beam: an oscillation of the beam centroid along its length [19]. Ultimately, the bunch tail hits the wall of the channel and the bunch is destroyed. The characteristic growth distance of the BBU instability is sufficiently short that no significant energy exchange from the driver to the wake can be achieved before the driver is lost. A similar instability is observed in dielectric-based accelerators [7].

BBU is well known in conventional linear accelerators [20]. There, it is controlled through BNS-stabilization [21], in which an energy chirp is applied to the bunch. The resulting head-to-tail chirp in the betatron frequency breaks the resonance between the beam and channel, suppressing the instability. The chirp must be consistent with the focusing properties of the quadrupole guiding structure [22], and must be maintained over the whole accelerating/decelerating distance. Recently, BNS stabilization has been successfully applied to dielectric-based accelerating structures [23]. However, even with current state-of-the-art magnetic quadrupole technology, offering field gradients on the order of 1 T/mm, the attainable accelerating field is limited to a few 100 MV/m.

Here we show that stable acceleration in a hollow plasma channel can be achieved through the inclusion of a thin co-axial plasma filament. The accelerator configuration is shown in Fig. 1. We assume the plasma density n in the filament to be the same as in the walls of the channel. The filament radius r_f must be small, so that $k_p r_f \ll 1$. Here $k_p = \omega_p/c$ is the characteristic plasma wave number, with $\omega_p = \sqrt{4\pi n e^2/m}$ is the corresponding electron plasma frequency. If we use an electron drive bunch with a current $I_d \gg I_A (k_p r_f)^2$, where $I_A = mc^3/e = 17$ kA is the natural current unit, the transverse self-field of the driver will scatter the plasma electrons from the filament. The remaining ion column will guide both the electron driver and a negatively charged witness. Simultaneously, the ion column will slowly pinch due to the high charge of the drive beam. The characteristic pinch time is $\tau_i \sim (r_f/c) \sqrt{M I_A / Z m I_d}$, where M is the ion mass and Z is the ion charge. As the ion pinch begins at the head of the driver, the ion density, and so the effective betatron frequency, increases along the length of the beam. This chirp is independent of the beam energy, allowing much larger chirp rates than can be achieved by tailoring the driver energy. The large effective chirp guarantees the bunch stability through the BNS mechanism [21, 22], even for a monoenergetic driver.

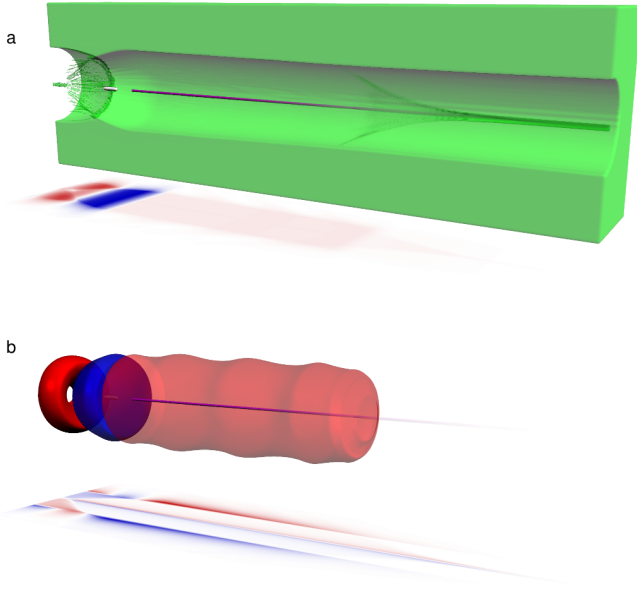


Figure 1. Configuration of the co-axial-channel accelerator. a) A drive beam (purple) propagates in a hollow channel, scattering the plasma electrons (green) from the co-axial filament. The response of the bulk plasma generates an electric field, shown as a 2D cut through the axis projected underneath. This field allows the acceleration of a witness bunch (white) to energies much higher than that of the driver. b) Field configuration, showing isosurfaces of the decelerating field acting on the driver (translucent red, at $0.01E_c$, where $E_c = c\omega_p m/e = 22$ GV/m); the accelerating field acting on the witness (blue, $-0.1E_c$); and the field suitable for the acceleration of positrons (red, $0.1E_c$). The projection underneath shows a 2D cut through the axis of the transverse force $E_y - B_z$ acting on the driver and witness.

To demonstrate stable acceleration in a co-axial channel, we use the fully three-dimensional quasi-static particle-in-cell code qv3d, developed on the platform of the VLPL code [24]. We choose helium as the background gas with an atomic density $n = 5 \times 10^{16} \text{ cm}^{-3}$. The hollow plasma channel has a radius $k_p r_c = 3$, and the on-axis plasma filament has a radius $k_p r_f = 0.2$. In dimensional units, these are $r_c = 71 \mu\text{m}$ and $r_f = 4.8 \mu\text{m}$. The filament and channel walls are taken to be singly ionized. We do not discuss here how such a plasma configuration may best be achieved. The standard method to create a hollow channel is by laser ionization [6]. The co-axial filament could, for example, be ionized by a higher-order laser mode or even by the self-field of the drive bunch [25].

Both the driver and witness have an initial particle energy of 2 GeV. The driver consists of two bunches. The main driver has a ramped density profile, with a current increasing from zero to 10 kA over $570 \mu\text{m}$, and a Gaussian transverse profile with $\sigma_\perp = 1.7 \mu\text{m}$. The bunch duration is approximately equal to the characteristic pinch time for the ion column.

Such ramped density profiles minimize the decelerating field acting on the driver [26], allowing a larger transformer

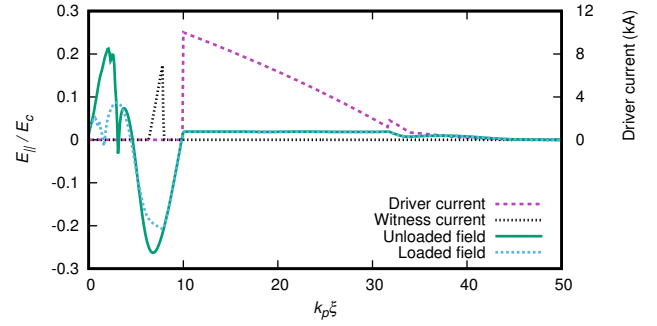


Figure 2. Beam profiles and wakefields. Initial drive- and witness-beam currents and the on-axis longitudinal field, plotted in the co-moving coordinate $\xi = z - ct$. The maximum decelerating wakefield inside the drive beam is $E_- = 0.019E_c$. The maximum unloaded accelerating field reaches $E_+^{\text{unloaded}} = -0.26E_c$, corresponding to an unloaded transformer ratio of 13.6. When loaded with the witness bunch, the accelerating field flattens to $\langle E_+^{\text{loaded}} \rangle = -0.2E_c \approx 4.3$ GV/m.

ratio. However, the high-current driver used here modifies the equilibrium radius of the channel, increasing the plasma density in the channel walls. This results in a larger accelerator loss factor [5], i.e. a stronger coupling between the drive beam and the channel. The optimal gradient for the main drive bunch is therefore lower than for a constant loss factor. We here make use of a logarithmic ramp profile $I(x) \sim \log(1 + \alpha x/L)$, with $\alpha = 0.057$, which corresponds to a first-order correction to the plasma response.

An additional nonlinear wake term arises due to the scattering of electrons from the on-axis filament. This increases the decelerating field near the leading edge of the driver, reducing the transformer ratio obtained from commonly-used driver profiles, e.g. the double-triangular bunch [27]. We avoid this limitation through the use of a second drive bunch which precedes the main driver, scattering the filament electrons before the peak decelerating field is reached. The leading bunch has a Gaussian rise, $\sigma_\parallel = 120 \mu\text{m}$, with a sharp cut to zero at its peak of 610 A. The transverse profile is the same as the main driver. The two drive bunches partially overlap, with the start of the main driver $53 \mu\text{m}$ before the peak of the preceding bunch.

The combined current profile of the two drive bunches, and the resulting wakefield, is shown in Fig. 2. The maximum decelerating field is $E_- = 0.019E_c$, where the critical field $E_c = c\omega_p m/e = 22$ GV/m for the chosen plasma density. The field structure has an unloaded transformer ratio $T_R = 13.6$. This value is 86% of the theoretical maximum for a main drive bunch of this length [28]. We note that the decelerating field after the peak is flat to within $\pm 2.3\%$. Further optimization would require a higher-order treatment for the plasma response.

The leading edge of the witness is located $49 \mu\text{m}$ behind the rear edge of driver. Its transverse profile is Gaussian with $\sigma_\perp = 1.2 \mu\text{m}$, and a peak current of 7 kA at its leading edge, decreasing linearly over its $36 \mu\text{m}$ length. This

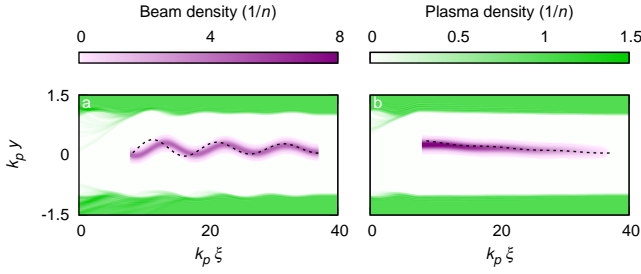


Figure 3. BBU instability. Comparison of the qv3d code (color-map) with a semi-analytical model (black dashed line) for BBU growth in the absence of a co-axial filament. A flat-top (a) and ramped (b) drive beam of average current 200 A propagate $Lk_p = 600$ in a channel of radius $r_{ck_p} = 1$. The instability is seeded by offsetting the driver by $0.05/k_p$ from the channel axis.

density profile is chosen to correctly load the wakefield. The average accelerating field experienced by the witness $\langle E_+ \rangle = -0.2E_c$ corresponds to a loaded transformer ratio $T_R = 10.2$.

Without the co-axial plasma filament the driver rapidly becomes transversely unstable. The BBU growth observed in the qv3d code is in good agreement with analytical models, as seen in Fig. 3, which compares simulations with the numerical solution of Eq. (13) from reference [5]. The results diverge as the plasma response becomes nonlinear due to the limitations of the analytic model, for example in wider channels as the influence of phase mixing becomes stronger [29]. For the parameters used in Fig. 1, BBU results in the loss of the witness beam over distances as short as $L_{BBU} \approx 4000k_p^{-1} \approx 10$ cm, limiting the energy gain to ~ 400 MeV.

The presence of the co-axial plasma filament, however, stabilizes the system so that BBU is avoided completely. We follow the acceleration over a total distance of $L_{acc} = 2 \times 10^5 k_p^{-1} \approx 4.8$ m. The phase-space evolution of the driver is shown in Fig. 4a. We observe that at the end of the acceleration length, the driving bunches have lost $\sim 86\%$ of their total energy.

The phase-space evolution of the witness bunch is shown in Fig. 4b. The witness initially develops a negative energy chirp, in agreement with the field at $L = 0$ shown in Fig. 2. However, as the witness is accelerated, it dephases with the drive beam, and so experiences a non-constant accelerating field over the acceleration length. As we carefully tuned the initial parameters, the gradient of the accelerating field acting on the witness is reversed after an acceleration length of ~ 3 m, reducing the chirp.

Figure 4c shows the energy spectra of the witness bunch. The energy spread initially increases due to the chirp, and subsequently decreases, reaching a near-monoenergetic peak at $W \approx 21$ GeV for an acceleration distance of $L = 4.8$ m. This corresponds to a total energy gain of 8.5 J. Given the initial drive-beam energy of 21 J, this represents a 40% efficiency. Comparing only the energy lost by

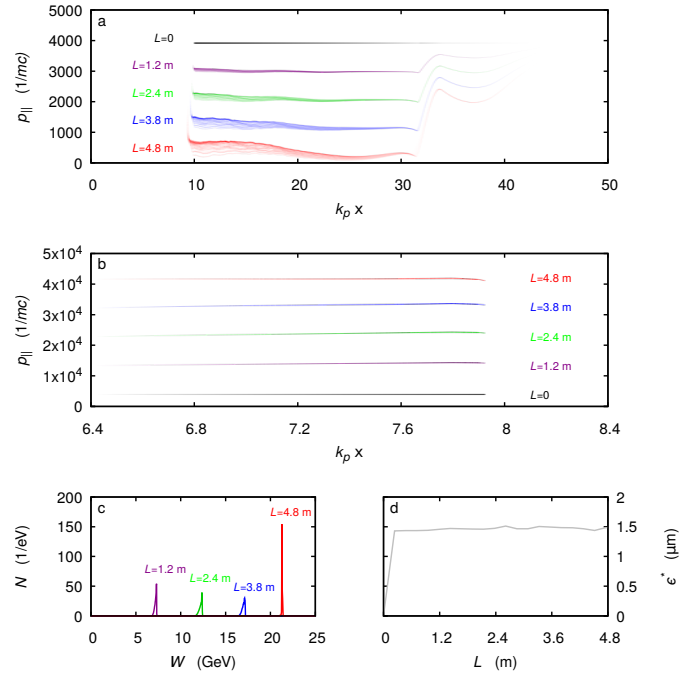


Figure 4. Evolution of the drive and witness beams. a) Longitudinal phase-space density ($p_{||}, \xi$) of the driver after an acceleration length of $L = 0$ (initial distribution), 1.2, 2.4, 3.6, and 4.8 m. At the end of the acceleration, the driver has lost a large fraction of its energy. b) Longitudinal phase space ($p_{||}, \xi$) of the witness at the same positions. Initially, the witness develops a longitudinal chirp. As the witness dephases with the driver, however, the field acting on the witness changes, leading to a reduction in the acquired chirp after ~ 3 m. c) Energy spectra of the witness bunch after an acceleration length of $L = 1.2, 2.4, 3.6$ and 4.8 m. The choice of initial witness parameters results in a near-monoenergetic bunch at the end of the acceleration length. d) Evolution of the witness bunch emittance over the entire simulation length. The large initial growth in emittance is likely numerical in nature.

the driver gives a transfer efficiency of 46%. The measured energy spread $\Delta W = 0.2\%$ is limited by the simulation resolution.

The normalized emittance of the witness grows rapidly at the start of the simulation to $\epsilon^* = 1.4 \mu\text{m}$, and then stays roughly constant over the entire acceleration length, as seen in Fig 4d. The rapid growth of the initial emittance is likely numerical in nature, with the resolution-limited emittance of the simulation estimated at $6 \mu\text{m}$.

Due to the use of an ion-column to focus the beam, this mechanism is only appropriate for an electron driver. However, we note that this configuration could be used to accelerate a positron witness bunch with a donut profile, as can be seen from the field configuration in Fig. 1. As the driver is many times longer than the witness, the effective chirp of the driver alone should be sufficient for stabilisation. We save a detailed investigation of this configuration for future work.

The ability to stably and efficiently accelerate a witness

bunch in a plasma channel finally offers a path towards a new generation of novel high-energy accelerators. The combination of high transformer ratio and monoenergetic acceleration potentially makes this technology a serious contender for applications-driven research.

METHODS

Simulations were carried out with the qv3d code [24]. The main simulation (Figs. 1,2,4) was carried out with a resolution of $\Delta_x = \Delta_y = 0.07/k_p$, $\Delta_z = 0.1/k_p$, and a simulation box size of $15/k_p \times 15/k_p \times 50/k_p$. The plasma response was modelled with a timestep $\Delta_t = 1000/\omega_p$, with the witness and drive beams subcycled with a timestep $\Delta_t = 10/\omega_p$ in order to correctly resolve the betatron frequency. 4 particles per cell were used for the bulk plasma, 64 for the drive beam and plasma filament, and 4096 for the witness bunch.

For the parameters used in this work, the peak drive current of 10.2 kA results in an increase in the equilibrium channel radius of $\sim 12\%$. This leads to an increase in the equilibrium electron density, n_{eq} . The effect can be estimated analytically. To first order, the increase in density varies linearly with the driver current, valid for the small perturbation to the radius observed here. This gives a first-order approximation for the accelerator loss factor $\kappa'/\kappa \sim n_{eq}/n \sim 1 + \alpha I$ [5]. The optimal current gradient for a ramped driver satisfies:

$$\frac{\partial I}{\partial x} \sim \frac{1}{\kappa'_0(x)} \sim \frac{1}{1 + \alpha I/I_{max}},$$

i.e. a logarithmic scaling for the current profile. Assuming the electron perturbation is limited to one skin depth gives $\alpha = 0.051 \text{ kA}^{-1}$. The optimal value found from simulations and used in this work is $\alpha = 0.056 \text{ kA}^{-1}$.

The optimal transformer ratio was calculated using the relation $T_R \leq \sqrt{1 + L^2 k^2}$ [28]. We here use the length L of the ramped drive bunch, and take k as the resonant wavenumber for the monopole mode for a hollow channel of this radius, $k = 0.66k_p$ [5]. This gives an optimal transformer ratio of 15.9.

Simulations of beam hosing in Fig. 3 were carried out for a drive beam of length $29/k_p$ with a Gaussian transverse profile $\sigma_\perp = 0.07/k_p$. A cell size of $0.025/k_p \times 0.025/k_p \times 0.025/k_p$ was used in order to give a similar number of cells across the channel width as the main simulation. The simulation box size was $6/k_p \times 6/k_p \times 40/k_p$, and both the plasma and beams were simulated with a timestep $\Delta_t = 10/\omega_p$. The plasma was simulated with 16 particles per cell, and other parameters were as for the main simulation. The semi-analytic solution was calculated by solving Eq. (13) in reference [5] numerically, with arbitrarily small time and spatial step, assuming the driver energy remains constant over the time taken for the instability to develop.

The driver and witness beams have a total charge of 10.7 nC and 443 pC, respectively, corresponding to initial

total energies of 21.4 J and 906 mJ. After an acceleration length of 4.8 m, they have energies of 2.89 and 9.43 J. This corresponds to an 86% depletion of the driver, and a witness energy gain of 8.53 J. The latter corresponds to 40% of the initial driver energy, or 46% of the energy lost by the driver.

The normalized transverse emittance is calculated from the macroparticle phase space. An accurate treatment requires that the particle weight w be taken into account, such that

$$\epsilon_x^* = \gamma \sqrt{\frac{(\sum w x^2)(\sum w x'^2) - (\sum w x x')^2}{(\sum w)^2}}.$$

Here, x is the transverse displacement from the weighted mean transverse position, and $x' = p_x/|p|$ is the deviation from the weighted mean angle. We take the total transverse emittance to be the geometric mean of the emittance in x and y .

Numerical Cherenkov radiation can lead to nonphysical emittance growth in standard Yee-like PIC codes [30]. However, the quasistatic nature of the qv3d code makes it naturally free from this numerical artefact. The minimum emittance that can be accurately modelled is therefore limited only by the simulation resolution. To calculate this limit, we consider a particle beam focused down to some radius x_0 . Particles oscillate at the betatron frequency, and we assume the particles are uniformly distributed over all phases. The normalized transverse emittance is then $\gamma \sqrt{\langle x^2 \rangle \langle x'^2 \rangle} = \gamma \sqrt{(x_0^2/3)(\omega_\beta^2 x_0^2/c^2)} = (\omega_\beta \gamma / \sqrt{3} c) x_0^2$. Choosing $\gamma = 4 \times 10^4$ and a beam diameter of one cell, $x_0 = 0.5 \Delta_x = 0.035/k_p$, and noting from simulations that the ion column density at the position of the witness is $\sim 6n$, the resolution limit for the normalized transverse emittance is $\sim 6 \mu\text{m}$.

REFERENCES

- [1] Esarey, E., Schroeder, C. B. & Leemans, W. P. Physics of laser-driven plasma-based electron accelerators. *Rev. Mod. Phys.* **81**, 1229–1285 (2009).
- [2] Joshi, C. & Caldwell, A. Plasma accelerators. In Myers, S. & Schopper, H. (eds.) *Accelerators and Colliders*, chap. 12.1, 592–605 (Springer Berlin Heidelberg, Berlin, Heidelberg, 2013).
- [3] Kimura, W. D., Milchberg, H. M., Muggli, P., Li, X. & Mori, W. B. Hollow plasma channel for positron plasma wakefield acceleration. *Phys. Rev. ST Accel. Beams* **14**, 041301 (2011).
- [4] Thompson, M. C. *et al.* Breakdown limits on gigavolt-per-meter electron-beam-driven wakefields in dielectric structures. *Phys. Rev. Lett.* **100**, 214801 (2008).
- [5] Schroeder, C. B., Whittum, D. H. & Wurtele, J. S. Multimode analysis of the hollow plasma channel wakefield accelerator. *Phys. Rev. Lett.* **82**, 1177–1180 (1999).
- [6] Lindström, C. A. *et al.* Measurement of transverse wakefields induced by a misaligned positron bunch in a hollow

- channel plasma accelerator. *Phys. Rev. Lett.* **120**, 124802 (2018).
- [7] Li, C. *et al.* High gradient limits due to single bunch beam breakup in a collinear dielectric wakefield accelerator. *Phys. Rev. ST Accel. Beams* **17**, 091302 (2014).
- [8] Pukhov, A. & Meyer-ter Vehn, J. Laser wake field acceleration: the highly non-linear broken-wave regime. *Appl. Phys. B* **74**, 355–361 (2002).
- [9] Blumenfeld, I. *et al.* Energy doubling of 42 GeV electrons in a metre-scale plasma wakefield accelerator. *Nature* **445**, 741 (2007).
- [10] Rosenzweig, J. B. *et al.* Plasma wakefields in the quasi-nonlinear regime. *AIP Conference Proceedings* **1299**, 500–504 (2010).
- [11] Lu, W., Huang, C., Zhou, M., Mori, W. B. & Katsouleas, T. Nonlinear theory for relativistic plasma wakefields in the blowout regime. *Phys. Rev. Lett.* **96**, 165002 (2006).
- [12] Golovanov, A. A., Kostyukov, I. Y., Thomas, J. & Pukhov, A. Beam loading in the bubble regime in plasmas with hollow channels. *Phys. Plasmas* **23**, 093114 (2016).
- [13] Pukhov, A. *et al.* Phase velocity and particle injection in a self-modulated proton-driven plasma wakefield accelerator. *Phys. Rev. Lett.* **107**, 145003 (2011).
- [14] Muggli, P. *et al.* Awake readiness for the study of the seeded self-modulation of a 400 gev proton bunch. *Plasma Phys. Controlled Fusion* **60**, 014046 (2018).
- [15] Andreev, N. E., Gorbunov, L. M., Kirsanov, V. I., Nakajima, K. & Ogata, A. Structure of the wake field in plasma channels. *Phys. Plasmas* **4**, 1145–1153 (1997).
- [16] Yi, L. *et al.* Positron acceleration in a hollow plasma channel up to tev regime. *Sci. Rep.* **4**, 4171 (2014).
- [17] Behnke, T. *et al.* The International Linear Collider Technical Design Report - Volume 1: Executive Summary. Tech. Rep., The International Linear Collider (2013).
- [18] Tschentscher, T. *et al.* The European X-ray Free-Electron Laser facility: A new infrastructure for research using ultrashort, coherent x-ray pulses of extreme brightness. *Synchrotron Radiation News* **19**, 13–19 (2006).
- [19] Whittum, D. H., Sharp, W. M., Yu, S. S., Lampe, M. & Joyce, G. Electron-hose instability in the ion-focused regime. *Phys. Rev. Lett.* **67**, 991–994 (1991).
- [20] Panofsky, W. K. H. & Bander, M. Asymptotic theory of beam break-up in linear accelerators. *Review of Scientific Instruments* **39**, 206–212 (1968).
- [21] Balakin, V. E., Novokhatsky, A. V. & Smirnov, V. P. VLEPP: Transverse beam dynamics. In *Proceedings, 12th International Conference on High-Energy Accelerators, HEACC 1983: Fermilab, Batavia, August 11-16, 1983*, vol. C830811, 119–120 (1983).
- [22] Stupakov, G. V. BNS damping of beam breakup instability. *SLAC-AP-108* (1997).
- [23] Zholents, A. *et al.* A preliminary design of the collinear dielectric wakefield accelerator. *Nuclear Instruments and Methods in Physics Research Section A: Accelerators, Spectrometers, Detectors and Associated Equipment* **829**, 190 – 193 (2016). (2nd European Advanced Accelerator Concepts Workshop - EAAC 2015).
- [24] Pukhov, A. Particle-in-cell codes for plasma-based particle acceleration. *CERN Yellow Reports* **1**, 181 (2016).
- [25] Tarkeshian, R. *et al.* Transverse space-charge field-induced plasma dynamics for ultraintense electron-beam characterization. *Phys. Rev. X* **8**, 021039 (2018).
- [26] Bane, K. L. F., Chen, P. & Wilson, P. B. On collinear wake field acceleration. *IEEE Transactions on Nuclear Science* **32**, 3524–3526 (1985). Also published in SLAC-PUB 3662 (1985).
- [27] Jiang, B., Jing, C., Schoessow, P., Power, J. & Gai, W. Formation of a novel shaped bunch to enhance transformer ratio in collinear wakefield accelerators. *Phys. Rev. ST Accel. Beams* **15**, 011301 (2012).
- [28] Baturin, S. S. & Zholents, A. Upper limit for the accelerating gradient in the collinear wakefield accelerator as a function of the transformer ratio. *Phys. Rev. Accel. Beams* **20**, 061302 (2017).
- [29] Shvets, G. & Li, X. Theory of laser wakes in plasma channels. *Physics of Plasmas* **6**, 591–602 (1999).
- [30] Lehe, R., Lifschitz, A., Thaury, C., Malka, V. & Davoine, X. Numerical growth of emittance in simulations of laser-wakefield acceleration. *Phys. Rev. ST Accel. Beams* **16**, 021301 (2013).

ACKNOWLEDGEMENTS

This work has been supported by the Deutsche Forschungsgemeinschaft and by BMBF.

AUTHOR CONTRIBUTIONS

The scheme was conceived by AP. Both authors contributed to simulations, data analysis and manuscript preparation.

COMPETING INTERESTS

The authors declare no competing interests.